Crises-induced intermittencies in a coherently driven system of two-level atoms

Carlos L. Pando L., Gabriel Perez,* and Hilda A. Cerdeira†
International Centre for Theoretical Physics, P.O. Box 586, 34100 Trieste, Italy
(Received 14 October 1992)

We study the coherent dynamics of a thin layer of two-level atoms driven by an external coherent field and a phase-conjugated mirror (PCM). Since the variables of the system are defined on the Bloch sphere, the third dimension is provided by the temporal modulation of the Rabi frequencies, which are induced by a PCM which reflects an electric field with a carrier frequency different from the incident one. We show that as the PCM gain coefficient is changed, period doubling leading to chaos occurs. We find crises of attractor-merging and attractor-widening types related to homoclinic and heteroclinic tangencies, respectively. For the attractor-merging crisis we find the critical exponent for the characteristic time of intermittency versus the control parameter which is given by the gain coefficient of the PCM. We show that during the crisis of attractor-widening type, another crisis due to attractor destruction occurs as the control parameter is changed. The latter is due to the collision of the old attractor with its basin boundary when a new attractor is created. This new attractor is stable only in a very small interval in the neighborhood of this second crisis.

PACS number(s): 05.45.+b,42.65.−k

I. INTRODUCTION

There has been an increasing interest in the dynamics of thin layers of two-level or multilevel atoms interacting with driving fields [1–4]. In this article we present a study of the chaotic behavior that occurs in a system consisting of a thin layer of two-level atoms interacting with an external coherent field and a phase-conjugated mirror. Here we use the semiclassical, rotating-wave and plane-wave approximations [5]. Since we neglect any coupling with a reservoir we study the long-term dynamics of this coherent system. In Ref. [6] collective decay or excitation of a point sample of two-level atoms was analyzed. A further reformulation and extension of this problem was given in article [4], where the case of exact resonance (one mode approximation) was studied. Here we analyze the case when the phase-conjugated mirror reflects a field with a carrier frequency different from the incident one. It is precisely this frequency mismatch that makes the system time dependent, i.e., explicit time-dependent Rabi frequencies appear which drive the system of two-level atoms periodically. The variables of the differential equation describing this optical system lie on a sphere. Therefore the system has a three-dimensional phase space: two dimensions due to the sphere and the explicit periodic time dependence in the equations. As a result chaos may occur. In particular, we study crises that appear in this system. Crises taking place in dissipative diffeomorphisms on the sphere had been studied to a lesser extent than in driven dissipative systems on the plane such as the Van der Pol oscillator [7].

In a crisis a sudden change in the dynamics of a chaotic attractor occurs as a control parameter is changed [8, 9]. More specifically, these sudden changes may have three forms. The first, called attractor destruction, refers to the disappearance of a chaotic attractor. The attractor becomes just a chaotic transient. The second type of crisis, known as attractor widening, corresponds to a discontinuous change in the size of a chaotic attractor with random bursts between the old and new region occupied by the attractor. Finally, the third one, called attractor merging, refers to the merging of two or more existing attractors to form a single attractor [8,9]. An alternative to study these phenomena is in terms of the characteristic time for a given crisis [8, 9]. The validity of the scaling behavior for the characteristic time in the vicinity of crises had been confirmed in recent experiments [10, 11].

In Sec. II we present a set of equations that describe our optical system, stressing the way our equations differ from those of Ref. [4]. In Sec. III two fundamental symmetries of the system are established. We show a bifurcation diagram for the variables of the system sampled at every driving period versus the control parameter that is given by the gain coefficient of the phase-conjugated mirror (μ). Poincaré sections are shown which give us some insight into the crisis phenomena that we consider. In Sec. IV we study two successive crises that occur in our system as μ is changed. We show that the first crisis is related to a homoclinic tangency between the stable and unstable manifolds. We calculate the critical exponents which are related to the average switching time between different attractors in an attractor-merging crisis. Further, the plots of the Lyapunov exponents as a function of μ are given. The second crisis is shown to be related to a heteroclinic tangency of manifolds. Here we find that a new chaotic attractor appears which destroys the old attractor. This attractor is related to the onset of new tangencies of the invariant manifolds. In Sec. V we give the conclusions.

II. GENERAL THEORY

Here we show the equations that describe the interaction between a system of two-level atoms pumped si-

multaneously by a phase-conjugated mirror (PCM) and by an external coherent field. In Ref. [4] the case of exact resonance between the frequencies of the external field, the transition frequency of the two-level atoms and phase-conjugated mirror pump fields, has been studied. There it was assumed that the PCM is produced by four-wave mixing [12]. Here we analyze the case when the external field and PCM pump field frequencies are different. The latter lead us to time-dependent Rabi frequencies for the Bloch vector components, as we will see below. Next we give the equations stressing the way the time-dependent Rabi frequencies are obtained.

Let us consider the system shown in Fig. 1. The region $z \leq l \quad (l \geq 0)$ is occupied with a dielectric whose dielectric constant is ϵ, a PCM occupies the region $(z \geq l)$. A thin layer of two-level atoms with thickness $d \ll \lambda$, where λ is the wavelength of the emitted light by the atoms in vacuum, is centered parallel to the interface $(z = 0)$. We assume that the space between the atomic layer and the interface is $l \gg \lambda$ and that l is of the same order of magnitude of the distance from the atomic dipole to its radiation zone, so that retardation effects are negligible. A coherent applied field is incident perpendicularly upon the interfaces from the region $z < 0$. The field is a plane wave linearly polarized along the x axis tuned at exact resonance with the atoms. Taking into account the presence of the thin polarizing layer of two-level atoms, the boundary conditions at $z = 0$ are

$$\begin{aligned} &E_x(0^+,t) - E_x(0^-,t) = 0, \\ &H_y(0^+,t) - H_y(0^-,t) = -\frac{4\pi}{c}\frac{\partial P_x}{\partial t}. \end{aligned} \tag{1}$$

Here $E_x(z,t)$ and $H_y(z,t)$ are the components of the electromagnetic field [13], and P_x is the surface polarization of the atomic thin film. The boundary conditions at $z = l$ will be written below. The electric fields and the polarization have the following form for $z < 0$:

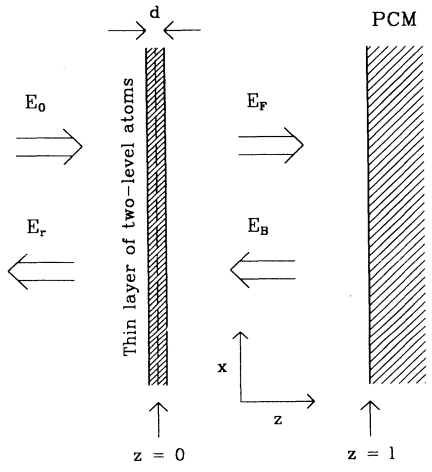

FIG. 1. Schematic representation of a thin layer of two-level atoms interacting with an external laser field E_0 and a phase-conjugated mirror (PCM).

$$E_x^{(1)}(z,t) = \frac{1}{\sqrt{2}}\{\, E_0(z,t)\exp[i(kz-\omega t)] + E_r(z,t)\exp[-i(kz+\omega t)] + \text{c.c.}\},$$

while for $0 < z < l$ we obtain:

$$E_x^{(2)}(z,t) = \frac{1}{\sqrt{2}}\{\, E_f(z,t)\exp[i(kz-\omega t)] + E_b(z,t)\exp[-i(kz+\omega t)] + \text{c.c.}\},$$

and

$$P_x = \frac{1}{\sqrt{2}}[P\exp(-i\omega t) + \text{c.c.}]. \tag{2}$$

Here $E_0(z,t)$, $E_r(z,t)$, $E_f(z,t)$, $E_b(z,t)$, and P are the slowly varying envelopes of the incident, reflected, forward, backward, and polarization fields, respectively, and $k = \omega\sqrt{\epsilon}$.

At the interface $z = l$ the phase-conjugated mirror produces a reflected wave E_{PCM} whose amplitude is defined as follows [12]:

$$E_{\text{PCM}} = E_b\exp(-ikl) = \mu[E_f\exp(ikl)]^*, \tag{3}$$

where $\mu = |\mu|\exp(i\psi)$, $|\,\mu\,|$ stands for the PCM gain coefficient, the phase ψ is a time-dependent function and is given by $\psi = \psi_0 + \delta t$, where ψ_0 is the PCM intrinsic phase [12], and δ is the frequency mismatch between the carrier frequency of the external driving field ω and the carrier frequency of the conjugate field ω_b $(\delta = \omega_b - \omega)$. The processes that may produce this mismatch are four-wave mixing and stimulated Brillouin scattering. If the PCM was created by four-wave mixing then the conjugated field E_b would have a carrier frequency $\omega_b = \omega_1 + \omega_2 - \omega$, according to the conservation of photon energy in this process. Here ω_1 and ω_2 are the frequencies of the pump fields. We assume that the conjugated field E_b propagates in opposition to the incident probe field, following the conservation of photon momentum in this process [12]. In the case when the PCM is generated by stimulated Brillouin scattering, the conjugate field carrier frequency ω_b happens to be down-shifted due to the interaction between the forward coherent optical field and the acoustic wave in a nonlinear medium [12].

Following Ref. [4] we find the total electric field at the atomic layer position $(z = 0)$. This self-consistent field is inserted in the Bloch equations, which after a change of variables yield [4]

$$\begin{aligned} \frac{dX}{dt} &= \Theta_x XD + \Omega_x D, \\ \frac{dY}{dt} &= \Theta_y YD - \Omega_y D, \\ \frac{dD}{dt} &= \Theta_x X^2 - \Theta_y Y^2 - \Omega_x X + \Omega_y Y, \end{aligned} \tag{4}$$

where

$$\Theta_x = 1 - \mid \mu \mid,$$
$$\Theta_y = 1 + \mid \mu \mid,$$
$$\Omega_x = \Omega_0 \Theta_x \sin\left(\varphi - \frac{\psi}{2}\right),$$
$$\Omega_y = \Omega_0 \Theta_y \cos\left(\varphi - \frac{\psi}{2}\right),$$
$$\Omega_0 = \frac{2\chi}{g} \mid E_0 \mid .$$

Here D is the population inversion, X and Y are the slowly varying components of the atomic polarization. The external coherent field at $z = 0$ is written as $E_0 = \mid E_0 \mid \exp(i\varphi)$. The time has been renormalized $t \to gt$. g is the cooperative decay rate and χ is the atom-field coupling constant [4]. Here we assumed that the transition frequency between the upper and lower energy levels of the two-level atoms coincides with the carrier frequency of the external laser field ω. We consider the case when $\varphi = 0$, $\psi_0 = 0$ and δ is renormalized to $\delta = (\omega_b - \omega)/2g = (\omega_1 + \omega_2 - 2\omega)/2g$. In this way using the definition for ψ we obtain $\varphi - \psi/2 = -\delta t$. At exact resonance, i.e., when $\delta = 0$, these equations had been solved [4].

The equations studied in this work are a limit when the coupling of the two-level atoms and reservoir is neglected [4]. For a pure radiative process, defining the transversal decay rate by γ, one may find that the cooperative decay rate is $g \approx \gamma n$, where n is the surface atomic density. In this case the components of the Bloch vector would suffer an additional decay given by a purely linear damping term. By renormalizing the time $t \to gt$, as done here, the coefficients of these linear damping terms will scale as $\gamma/g \approx 1/n$. Assuming a big enough value for the surface atomic density n, the linear decay coefficients may be considered as a small perturbation in the system, as a result of which the qualitative dynamics of the system in an interval of the control parameter space μ is the same with or without linear damping terms. A more rigorous formulation of the conditions under which a small perturbation does not change qualitatively the dynamics of our system requires a study of the associated structural stability. We consider this study as a first step to analyze the more realistic case that takes into account the effect of the reservoir, since the theory of two-dimensional maps is much better understood than maps in higher dimensions.

Finally as regards the experimental feasibility of the present system, where the small linear damping terms might be included, it will be ideal that the experiment reproduce the general features of Fig. 1, as discussed in Ref. [4]. However, one may also consider situations where a system of two-level atoms is contained in resonant cavities working in the bad-cavity limit. These are millimeter-wave cavities containing Rydberg atoms where superradiant behavior has been observed [14] or ring cavities containing two-level atoms suited for superradiance [15]. However, here two important elements must be included. One is the external coherent field that is assumed to be in resonance with the atomic transition frequency and the cavity frequency. The other is the PCM that transforms the output field of the system and has to be reinjected in the resonant cavity. Let us point out that in the case of the millimeter-wave cavity the active atoms occupy a thin slab which has a width smaller than the millimeter wavelength [14], and therefore may be considered as a thin film of two-level atoms.

III. PROPERTIES OF THE EQUATIONS

From now on μ will stand for $|\mu|$. The system of equations (4) may be rewritten in the following way:

$$\begin{aligned}\frac{d\phi}{dt} &= -2\mu D\cos\phi\,\sin\phi + \Omega_x \frac{D}{\sqrt{1-D^2}}\cos\phi \\ &\quad + \Omega_y \frac{D}{\sqrt{1-D^2}}\sin\phi, \\ \frac{dD}{dt} &= -\Theta_x(1-D^2)\sin^2\phi - \Theta_y(1-D^2)\cos^2\phi \\ &\quad - \Omega_x\sqrt{1-D^2}\sin\phi + \Omega_y\sqrt{1-D^2}\cos\phi\end{aligned} \tag{5}$$

upon the following change of coordinates:

$$D = D,$$
$$X = \sqrt{1-D^2}\sin\phi,$$
$$Y = \sqrt{1-D^2}\cos\phi.$$

The instantaneous rate of change is given by the divergence of the flow:

$$\nabla \mathbf{f} \equiv \frac{\partial \dot{\phi}}{\partial \phi} + \frac{\partial \dot{D}}{\partial D} = 2D. \tag{6}$$

According to Eq. (6), volumes do not change uniformly everywhere in phase space. In fact, they may contract or even expand. On the average, however, they contract for the parameter values that we use as we shall discuss next. The limit of this average volume change Λ_0 is a definite quantity and equals the sum of the three Lyapunov exponents of Eqs. (5) when regarded as an autonomous system [16]

$$\Lambda_0 = \lim_{t\to\infty}\frac{2}{t}\int_0^t D(q)dq = \lim_{t\to\infty}\frac{2}{t}\xi = \lambda_1 + \lambda_2 + \lambda_3. \tag{7}$$

Since time flows uniformly one of the Lyapunov exponents, say λ_3, is equal to zero.

It is known that all strange chaotic attractors in a flow defined in a phase space of three dimensions have the same spectrum of Lyapunov exponents $(+, 0, -)$ [16, 17]. For periodic orbits the spectrum is $(0, -, -)$.

In Fig. 2(a) we see the attractor for $\mu = 2$, i.e., the Poincaré section of the flow of Eqs. (5) in the (ϕ, D) plane sampled every period of the Rabi frequencies Ω_x and Ω_y. In Figs. 2(b) and 2(c) the maximum Lyapunov exponent λ_1 and the Kaplan-Yorke dimension D_{KY} are shown as a function of time, i.e., the number of iterates. Near the crises dimension D_{KY} is the typical value for the attractors that we study. In these figures 50 000 points (orbits) had been plotted after a transient of 300 periods.

Equations (5) may be studied using the Poincaré mapping technique, i.e., we study the set of points generated by the intersection of the flow with the planes $t = nT$,

where $T = 2\pi/\delta = 2$. In Eqs. (5) there are two symmetries . The first symmetry S_1 is the following:

$$\begin{aligned} &D \to D, \\ &\phi \to \phi + \pi, \\ &t \to t + \frac{T}{2} = t + 1. \end{aligned} \tag{8}$$

The second symmetry S_2 is given by

$$\begin{aligned} &D \to -D, \\ &\phi \to -\phi, \\ &t \to -t. \end{aligned} \tag{9}$$

It means that under the operations of symmetry S_1 and

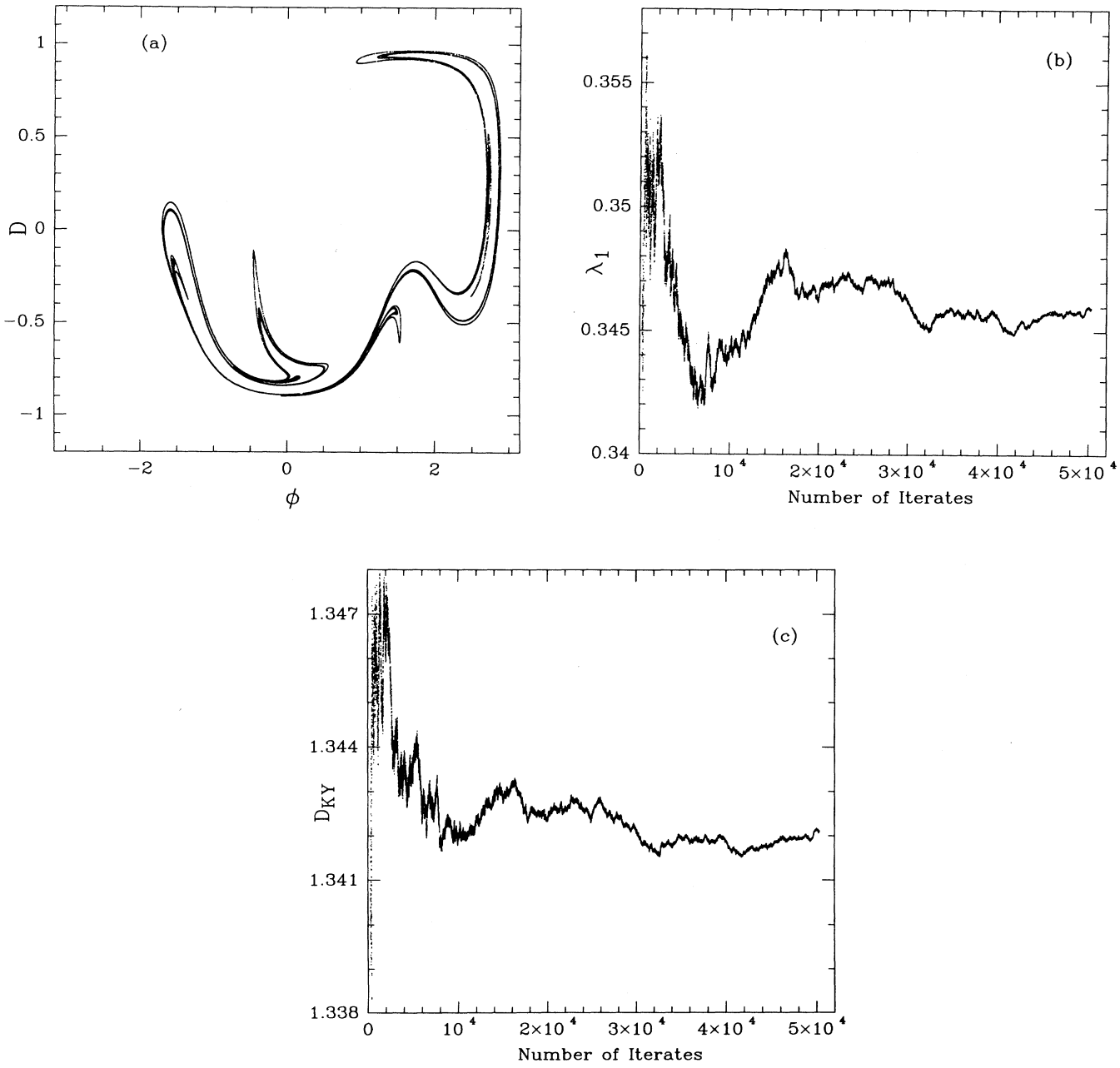

FIG. 2. Gain coefficient $\mu = 2.0$. In all these plots after a transient time of 300 periods the next 50 000 periods are considered. (a) Poincaré section (ϕ, D) of the flow given by Eq. (5) taken by sampling its solution every period of the Rabi frequencies Ω_x and Ω_y. (b) Transient for the maximum Lyapunov exponent λ_1 vs time (number of iterates). The limit at infinity gives λ_1. (c) Transient for the Kaplan-Yorke dimension D_{KY}.

S_2 the form of the equations does not change. In the present paper we study the transition to chaos by changing only one control parameter, namely, the parameter of nonlinearity μ. To this end we keep the parameter $\Omega_0 = 1$, which corresponds physically to an equality between the Rabi frequency (proportional to the external laser amplitude) and the collective damping coefficient g. Here the length of the Bloch vector has been normalized to 1. On the other hand, $\delta = (\omega_1 + \omega_2 - 2\omega)/2g = \pi$ we believe is not an unphysical estimate.

We study the behavior for $\mu > 1$, which means that the PCM reflects a field whose intensity is higher than the incoming one. We numerically checked that for $\mu < 1$ one has only periodic stable orbits. Let us point out that by definition the symmetry property S_2 of our dynamical system indicates that we are dealing with a reversible flow [18,19]. Several studies have been carried out recently on reversible flows or maps [20–22]. A typical property of reversible flows is the possible existence of conservative [Kol'mogorov-Arnol'd-Moser (KAM) tori] or dissipative (strange attractors) behavior in different regions of phase space. In particular a model for the CO_2 laser driven by an external coherent field shows this behavior [22]. Here the disappearance of conservative regions and the onset of dissipative structures are related to symmetry-breaking bifurcations. Near the crises and using grids with 300 different initial conditions each chosen randomly we always found that after a transient the orbit reaches an attractor. On the other hand, near the crises, all the period-1 orbits found on the sphere are saddles and their corresponding eigenvalues yield a product whose absolute value is less than 1. Therefore we conclude that we are dealing with a purely dissipative (reversible) system for which we apply the corresponding theory [16]. That, however, does not exclude the possibility that for other sets of parameters both conservative and dissipative behavior may coexist in our system. Considering the above symmetries we may more easily study the bifurcation diagrams shown in Figs. 3(a) and 3(b) for ϕ and D, respectively. Let us mention that the number of transients and the iterated points had been set equal to 300 and 400, respectively. This, according to our numerical calculations, is an optimum number of iterated points necessary to eliminate transients, except in the neighborhood of the critical values μ where crises arise and longer transients are required.

In the present system we have found that there are at most two possible basins of attraction for the selected parameters. In the case when there are two basins of attraction in the Poincaré section, say B_1 and B_2, with corresponding attractors A_1 and A_2, one may pass from A_1 (A_2) to A_2 (A_1) by applying the symmetry operation S_1 to any point of A_1 (A_2) and allowing the flow to have an evolution for half a period. However, when there is only one basin of attraction B with its corresponding attractor A, then the above-mentioned operation gives rise to a point that belongs to the same attractor A. Notice that the attractors mentioned above may be periodic or chaotic.

The second symmetry operation S_2 allows us to find the position of a saddle point $\mathbf{P}^*$, symmetric to a saddle point $\mathbf{P}$, such that $\mathbf{P}^* = (D^*, \phi^*) = -(D, \phi) = -\mathbf{P}$. Besides, upon the symmetry operation S_2 the dynamics backward in time is the same as the dynamics forward for Eqs. (5), but for a change in the sign of D and ϕ. That tells us that if we find a chaotic attractor which embeds a set of saddle points $\mathbf{P}_i = (D_i, \phi_i)$, $i = 1, \ldots, n$, then a repeller exists which embeds the symmetric set of points $\mathbf{P}^* = -(D_i, \phi_i)$, $i = 1, \ldots, n$. This repeller is in fact the inset (the stable manifold) of points $\mathbf{P}_i^*$, since in the dynamics backwards in time, this inset is the attractor [outset (unstable manifold)] for these points. Notice that these saddles may have arbitrary period.

To illustrate the latter we see in Fig. 4 the two different attractors A_1 and A_2 at $\mu_1^- = 1.945$ just before a crisis takes place. In Fig. 5 we see the only attractor and its corresponding repeller at $\mu_2^- = 2.04$ slightly before a second crisis occurs. Here after a transient of 300 periods, 5000 orbits were considered for each attractor or repeller.

According to the classification of crises given by Grebogi and co-workers [8,9], we could expect that for a critical value of $\mu = \mu_1$ such that $\mu_1^- < \mu_1$ attractor merging could occur, i.e., both attractors A_1 and A_2 at μ_1 form a single attractor A, as one may check by comparing Fig. 4 and the bifurcation diagrams given by Figs. 3(a) and 3(b).

On the other hand, at the critical value $\mu = \mu_2$ such that $\mu_2^- < \mu_2$ attractor widening could occur due to the collision of the only attractor A with the inset of the

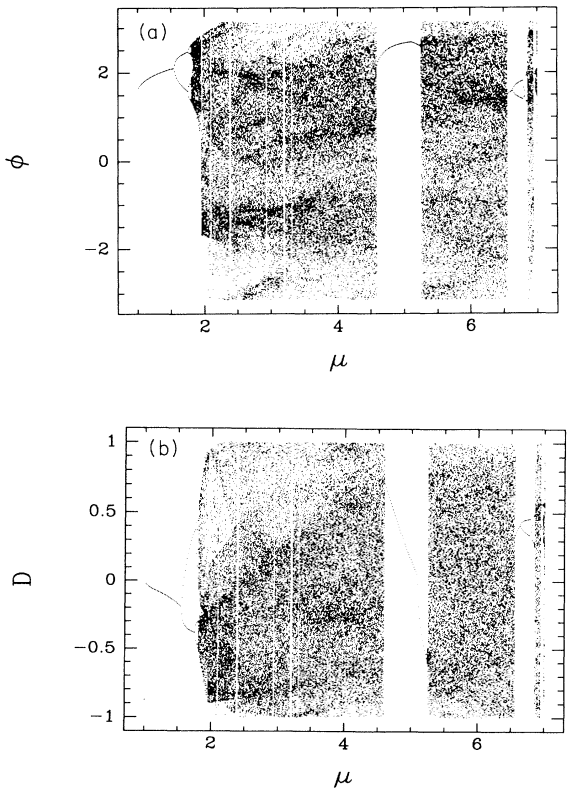

FIG. 3. Bifurcation diagrams for the azimuthal angle ϕ vs gain coefficient μ (a) and inversion D vs μ (b).

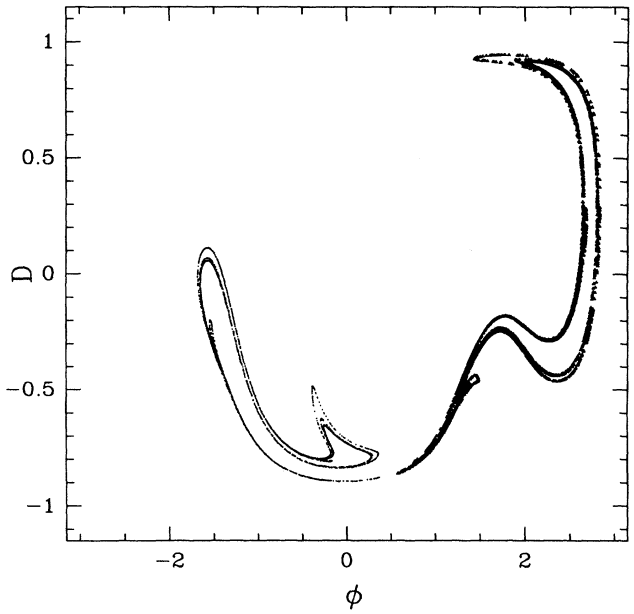

FIG. 4. Poincaré section for two different chaotic attractors A_1 (points) and A_2 (solid points) for $\mu = \mu_1^- = 1.945$, just before the first crisis occurs at $\mu = \mu_1$.

saddle points $\mathbf{P}_i^*$ (the repeller) symmetric to those points $\mathbf{P}_i$ embedded in the attractor. For μ values contained between μ_1 and μ_2 and their vicinities there are only six different period-1 saddle points in the Poincaré section. The above-mentioned crises-induced intermittencies will be treated in the next section.

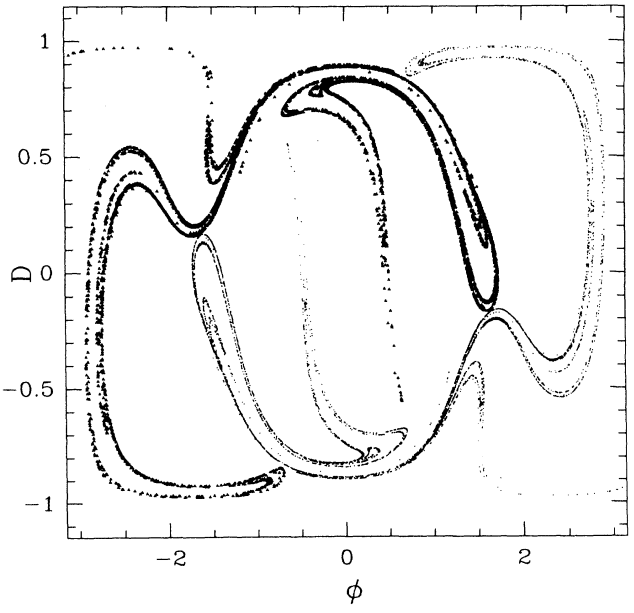

FIG. 5. Poincaré section for the only attractor A (points) and its repeller (solid points) for $\mu = \mu_2^- = 2.04$, just before the second crisis occurs at $\mu = \mu_2$.

IV. INTERIOR CRISES INDUCED BY THE PCM GAIN COEFFICIENT

In Fig. 6 we draw again for $\mu = 1.945$ all the period-1 saddle points, the unstable manifolds corresponding to the attractors A_1 and A_2, and the stable manifolds that form the basin boundary for the attractors A_1 and A_2. As it is clearly seen in Fig. 6 the formation of successive fingers (lobes) in the stable manifolds will give rise to an infinite sequence of homoclinic points [16]. At the first crisis ($\mu = \mu_1$) both attractors A_1 and A_2 touch simultaneously the boundary that separates their two basins. This is the signature of attractor merging [9]. The latter occurs because our system has the symmetry property S_1. In other words, any event happening to attractor A_1 (in particular, the boundary crisis) will occur with attractor A_2 which is obtained upon application of the symmetry S_1 to attractor A_1. Attractor A_2 reflects the dynamics of A_1 just half a period later.

For μ slightly larger than μ_1 the generated points will intermittently be localized in any of the former attractors, as suggested by Fig. 7 for ϕ versus time when $\mu = 1.96$. Similar intermittent pictures had been obtained for flows such as the forced damped pendulum [24] and the forced double-well Duffing equation [25]. In these cases two attractors merge to form a single attractor.

It has been proven by Young [26] that for two-dimensional invertible maps the information dimension D_I equals the Kaplan-Yorke dimension D_{KY}:

$$D_I = D_{\mathrm{KY}} = 1 + \frac{\lambda_1}{|\lambda_2|},$$

where λ_1 and λ_2 are the positive and negative Lyapunov

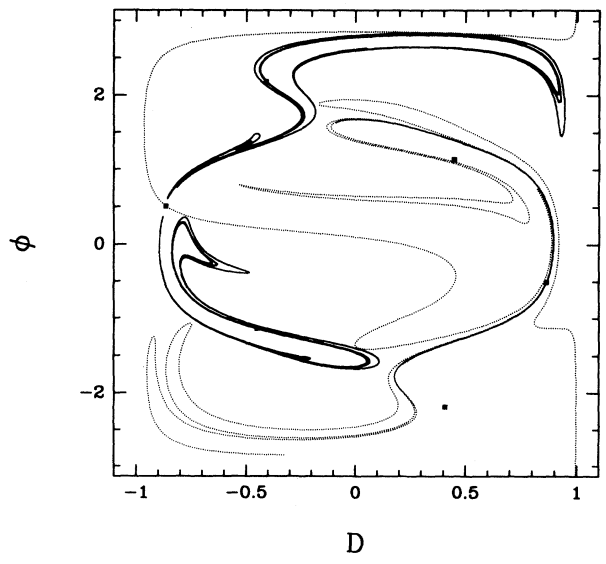

FIG. 6. For $\mu = \mu_1^- = 1.945$ we plot the single period unstable orbits (squares). Unstable manifolds of the saddles embedded in the chaotic attractor (solid lines). Stable manifolds of the saddles embedded in the basin boundary (dotted lines).

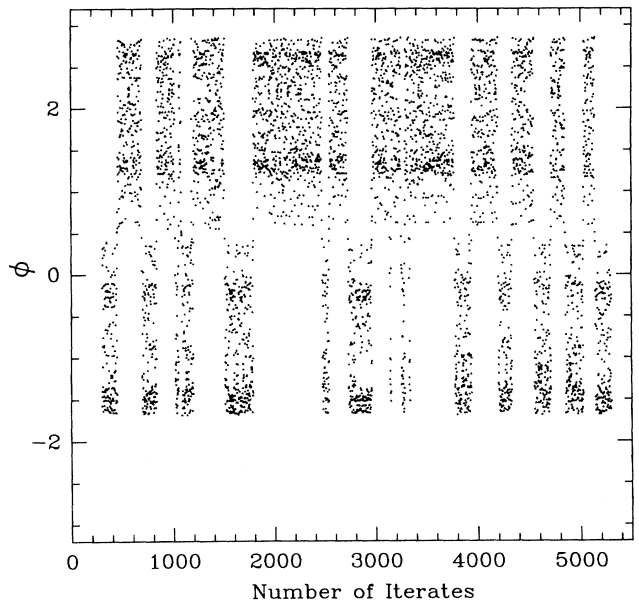

FIG. 7. For $\mu = 1.96 > \mu_1$, i.e., slightly after the first crisis, we plot the azimuthal angle ϕ vs the number of iterates.

exponents, respectively.

In Figs. 8(a) and 8(b) we show the bifurcation diagrams as μ is varied for the positive Lyapunov exponent λ_1 and the information dimension D_I. The transient time of λ_1 and D_I has been set equal to 8000 periods and only their values at the next 300 periods had been plotted for each μ value. The typical error we make in this plotting fluctuates between 1% and 0.1% of the real values of λ_1 and D_I. It happens since the temporal evolution of these quantities for this value of μ is similar to those when $\mu = 2.0$ as shown in Figs. 2(b) and 2(c).

In codimension-1 bifurcations, intermittencies due to crises of the type attractor merging or attractor widening cause a discontinuous jump in size of the chaotic attractor, in such a way that the chaotic attractor just before bifurcation lies inside the chaotic attractor just after bifurcation [23]. It has been stated, at least regarding differential equations having a smooth vector field, that the shift of dimension (measure) in attractor-merging or attractor-widening crises is continuous as we change a control parameter [23]. Accordingly, we believe that the behavior of D_I in terms of μ in Fig. 8(b) shows us that D_I changes continuously. However, as we will see next in the second crisis (attractor widening) D_I may vary discontinuously as a function of μ, though on the average D_I changes continuously. Sudden changes in the dimension of strange attractors by the eradication of a chaotic attractor by an infinitesimal change in a control parameter are called blue-sky catastrophes [7, 23] or attractor destruction [8, 9]. In this case the attractor becomes just a chaotic transient, i.e., the orbit leaves forever the region formerly occupied by the attractor for a control parameter larger than a certain critical value. For certain controls the Ikeda map [8] and the forced Van der Pol equation [7] show this behavior. In these cases the orbit goes to infinity.

Near a tangency between the stable and unstable manifolds the topology of the phase space changes. In particular, new attractors may appear (sinks), which might be periodic or chaotic. The number of these sinks may be finite or infinite. These sinks usually have very small basins of attraction [23, 27, 28]. It is worth mentioning that for the attractor-merging crises no sinks have been observed in the forced damped pendulum or in the forced double-well Duffing equation [9, 23]. Also in the blue-sky

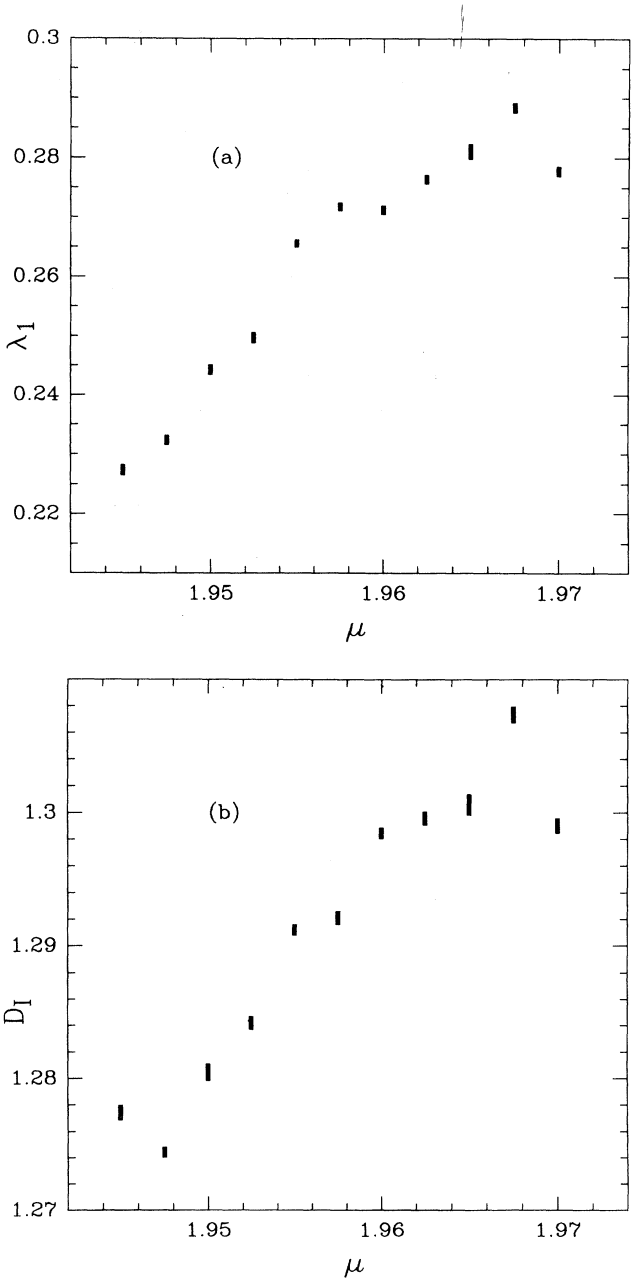

FIG. 8. Plots in the neighborhood of μ_1 (solid squares). (a) Maximum Lyapunov exponent λ_1 vs the gain coefficient μ. (b) Information dimension D_I vs μ. The transient time has been set equal to 8000 periods and only the last 300 iterates had been plotted.

catastrophe of a chaotic attractor, as in the attractor generated by the forced Van der Pol equation (Smale-Birkhoff attractor), when it loses stability approaching its basin boundary no additional new attractors (sinks) have been observed [7]. We believe that the destruction of the chaotic attractor in the crisis of attractor-widening type is due to the appearance of these sinks.

Notice that here the attractor-merging crisis is produced by a homoclinic event since the new tangencies are created only by the corresponding manifolds of the saddle point localized in the basin boundary. According to Grebogi and co-workers [9], past but near the homoclinic tangency one has the following scaling law:

$$T^* \sim (\mu - \mu_1)^{-\gamma},$$

where T^* in our case means the average time between switches of the two metastable attractors. In Fig. 9 we show a plot of $\ln(T^*)$ vs $\ln(\mu - \mu_1)$, together with the straight line that best fits this set of points. For each value of μ 10 000 periods had been considered after a transient time of 300 periods. The slope of the plotted straight line γ^* and its standard deviation $\Delta\gamma^*$ are given by

$$\gamma^* = 0.71,$$
$$\Delta\gamma^* = 0.17.$$

We have considered $\mu_1 = 1.951$. On the other hand, in Ref. [9] an expression is given for γ in terms of the eigenvalues $|\beta_-| < |\beta_+|$ of the saddle whose manifolds generate the new homoclinic tangencies:

$$\gamma = \frac{\ln(|\beta_-|)}{2\ln(|\beta_-\beta_+|)}. \tag{10}$$

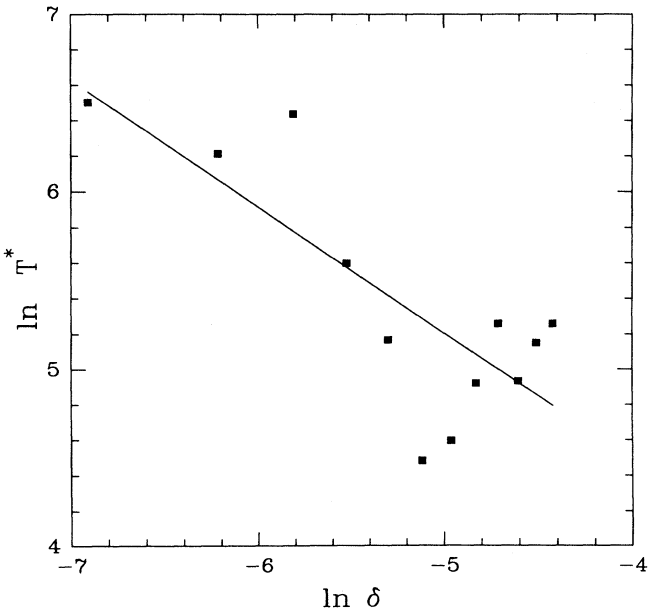

FIG. 9. Plot of $\ln(T^*)$ vs $\ln(\delta)$. Here $\delta = \mu - \mu_1$. T^* is the average time between switches among attractors A_1 and A_2 (solid squares). We show also the straight line that best fits this set of points. 10 000 periods had been considered to find T^* at every μ value.

For $\mu_1 = 1.951$ we found that $\beta_- = 0.006\,06$ and $\beta_+ = 5.217\,33$ and as a result $\gamma = 0.74$. Though one may see a good agreement among γ^* and γ, we believe that better statistics may improve the obtained results.

At the value $\mu = \mu_2$ with $2.04 < \mu_2 < 2.05$ a new crisis arises due to the collision of attractor A with its corresponding repeller (stable manifold) as suggested by Fig. 5. This type of crisis classified as attractor widening is similar to the intermittent bursting occurring in the Ikeda map for a certain set of controls [9]. There the unstable manifold of a period-5 orbit (the attractor) collides with the stable manifold of a different period-5 orbit. On the other hand, in our case beyond μ_1 we have only a single attractor A provided we are not too close to the tangencies of the manifolds. For $\mu = 2.06 > \mu_2$ the unstable and stable manifolds of the saddle points $\mathbf{P}_i$ and $\mathbf{P}_i^*$ respectively transversally intersect, as seen in Fig. 10. The similarity shared by the Ikeda map crisis of attractor-widening type [9] with this second crisis suggests to us that we have a heteroclinic tangency, since the new tangency is given only by the colliding stable and unstable manifolds that belong to different saddle points.

In Fig. 11 we plot as a function of μ in the neighborhood of μ_2 the largest Lyapunov exponent λ_1. Both quantities seem to change continuously as in the first crisis at $\mu = \mu_1$. The difference stems from the fact that here we observe a sharp decrease in the greatest Lyapunov exponent at $\mu_c = 2.046\,25$. For μ_c the temporal evolution of λ_1 during 100 000 periods is shown in Fig. 12 and the last 10 000 orbits of these series are plotted in Fig. 13, which we shall call attractor C. This attractor consists of five pieces.

The smooth curve in Fig. 12 that arises after a transient of roughly 6000 periods seems that it may be fitted according to the function

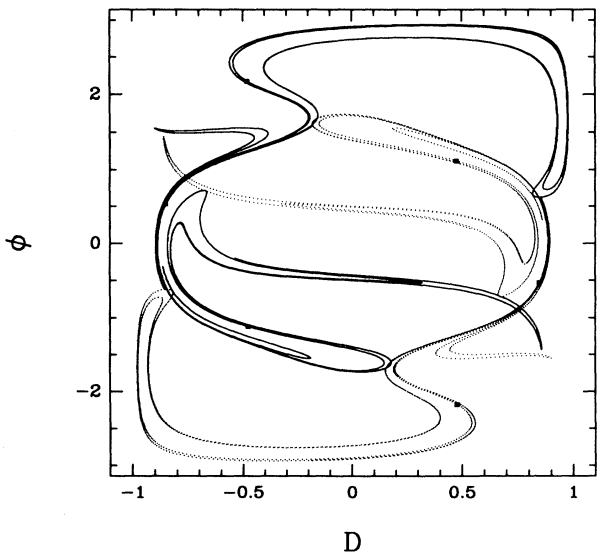

FIG. 10. For $\mu = 2.06$ transverse heteroclinic intersections among the unstable (solid line) and stable (dotted line) manifolds already occurs.

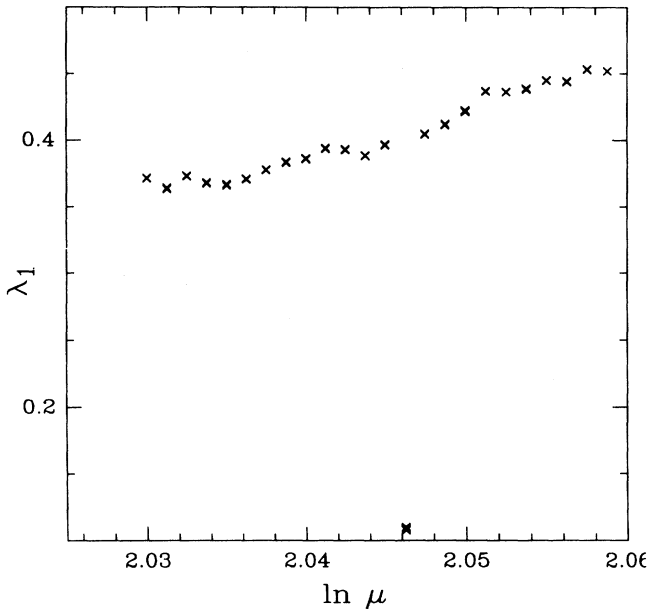

FIG. 11. Plot in the neighborhood of μ_2, for the maximum Lyapunov exponent λ_1 vs μ ($\times$).

$$\lambda_1 = \frac{c}{t^\alpha} + \beta \tag{11}$$

where c, α, and β are constants to be determined. If the smooth curve in Fig. 12 exactly fits that of Eq. (11) then the slope of the straight line

$$\ln[\lambda_1(t) - \beta] = \ln(c) - \alpha \ln(t) \tag{12}$$

in the plane $\ln(t)-\ln(\lambda_1-\beta)$ will give α for an appropriate value of β.

From Eq. (12) we may obtain an explicit equation for α:

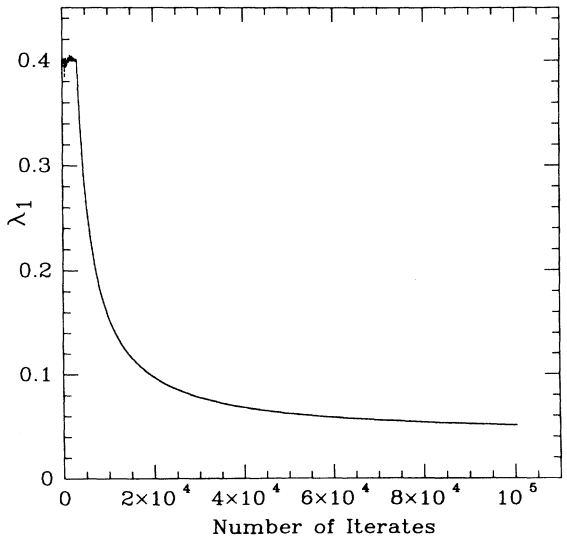

FIG. 12. Transient evolution for the maximum Lyapunov exponent λ_1 for $\mu = \mu_c = 2.046\,25$. 100 000 iterates are considered.

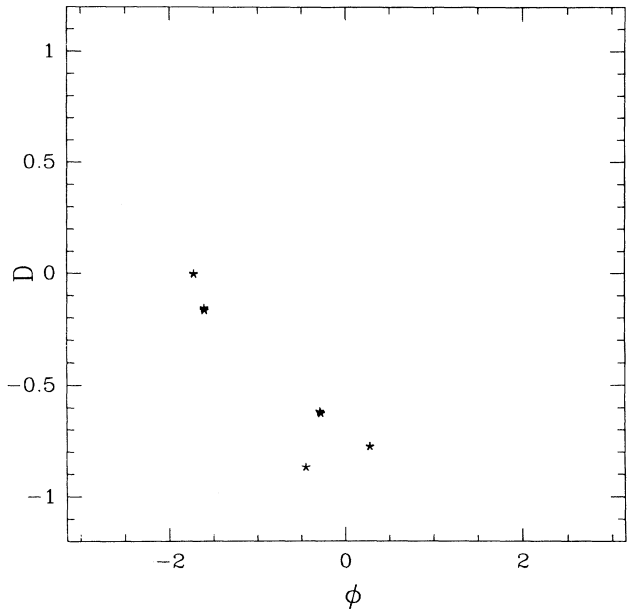

FIG. 13. Poincaré section of the chaotic attractor C ($\star$) for $\mu_c = 2.046\,25$. Another chaotic attractor $\tilde{C}$ is obtained upon application of the symmetry operation S_1.

$$\alpha = -\frac{\ln \frac{\lambda_1(t)-\beta}{\lambda_1(t_0)-\beta}}{\ln \frac{t}{t_0}}. \tag{13}$$

Here $t_0 = 6000$. Notice that for $t > t_0$ the hyperboliclike dependence of $\lambda_1(t)$ on time already has been settled. A plot of α as a function of β must give for the desired value of β a value for α with the least dispersion when all the values of t in Eq. (13) are considered. This is in fact the minimum requirement to obtain a nearly constant value of α. We find the optimum value $\beta = 0.0391$. For that value β we obtain an almost straight line for Eq. (12). This is shown in Fig. 14. A simple program for curve fitting of the set of points of Fig. 14 with a straight line gives the following parameters for α, $\ln(c)$ and their standard deviations $\Delta\alpha$ and $\Delta\ln(c)$:

$$\begin{aligned} \alpha &= 0.996\,38, \\ \Delta\alpha &= 6.67 \times 10^{-5}, \\ \ln(c) &= 7.0223, \\ \Delta\ln(c) &= 7.15 \times 10^{-4}. \end{aligned}$$

The obtained straight line basically coincides with that of Fig. 14. Therefore, according to the definition of Lyapunov exponent [16], the obtained value for $\beta > 0$ indicates that the rate of maximum exponential expansion (separation) of two nearby trajectories is nearly constant at any point on the attractor C. It is easy to prove that Eq. (11) may be simply rearranged in such a way that it matches the maximum Lyapunov exponent definition.

Here we would like to point out how the orbit falls into the attractor C. For $\mu = \mu_c$, after a short transient of around 300 periods the orbit enters for a long transient the region formerly occupied by the big attractor A until this orbit finally settles in attractor C. This mechanism

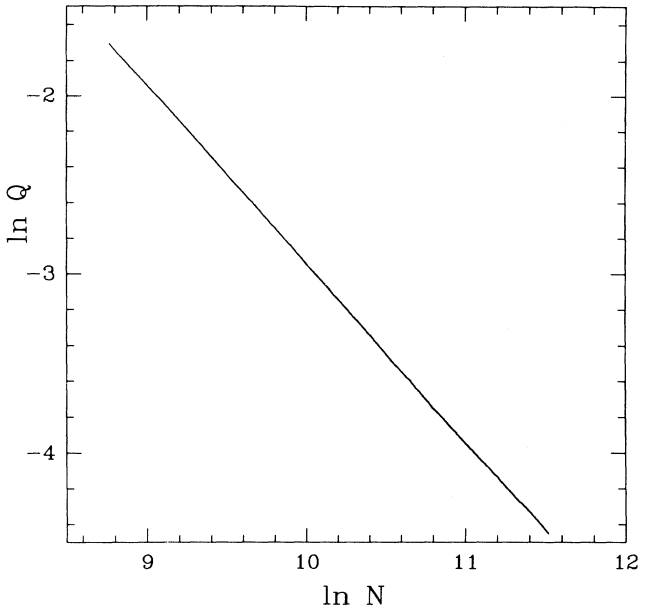

FIG. 14. Plot of $\ln(Q)$ vs $\ln(N)$. Here $Q = \lambda_1(N) - \beta$, N is the number of iterates (periods), and $\beta = 0.0391$.

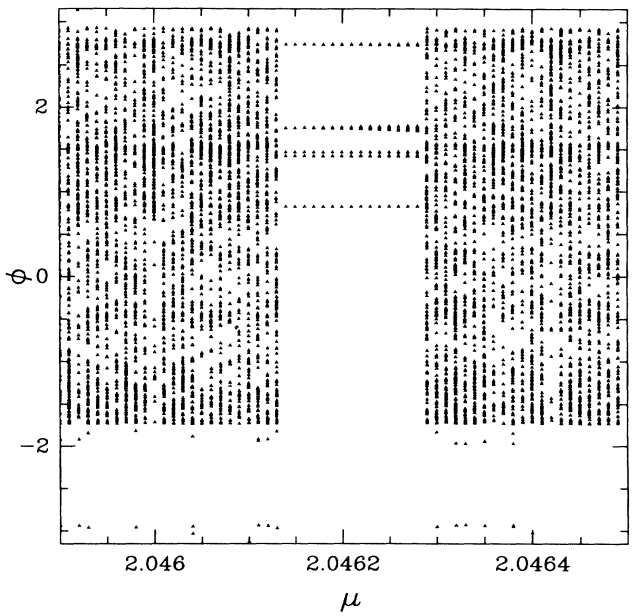

FIG. 15. Bifurcation diagram for the azimuthal angle ϕ vs μ .

occurs for all random initial conditions considered. As discussed above, at this moment the evolution of $\lambda_1(t)$ has a hyperboliclike dependence governed by Eq. (11). For $\mu = \mu_c$ attractor A is just a chaotic transient, since it is not anymore a set of recurrent orbits [27].

According to the numerical evidence that we show, we believe that at some value μ_{c1} the big attractor A touches its basin boundary created by the appearance of attractor C. The basin of attractor C must have very small dimensions, just prior to destruction of attractor A, since we do not detect attractor C for a large set of random initial conditions, in the vicinity of its basin at $\mu = \mu_c$. Here a crisis of the attractor-destruction kind occurs as suggested by Fig. 15. After a transient of 2000 periods, 200 orbits were plotted in the bifurcation diagram of Fig. 15 where, for μ values on the left- or right-hand side of this plot, attractor C does not exist and according to our numerical computations after a transient the orbit settles again in attractor A. For μ values in the vicinity of μ_c as shown in Fig. 15 any orbit in the phase space with the possible exception of a finite or infinite number of small basins will reach the attractor C. The transient time to reach attractor C depends strongly on the initial conditions.

For $\mu > \mu_c$, as μ is increased the period of attractor C also increases, eventually becomes chaotic and finally gets destroyed by colliding with its basin boundary. The last is a typical mechanism for destruction of an attractor. The existence of attractor C in a small interval near the second crisis is another reason that suggests to us that we are dealing with the above-mentioned sinks. Besides, it is known that these sinks must be localized near our attractor A, i.e., near the points of tangency of the invariant manifolds [28]. In fact, the destruction of attractor A by attractor C is possible due to the collision of attractor A with the small basin of attractor C. Therefore we have shown that not only are sudden jumps in size possible during a crisis of attractor-widening type but also sudden jumps in dimension due to the appearance of attractor C at the onset of a heteroclinic tangency. On the average the information dimension remains continuous. However, the sum of the Lyapunov exponents $\lambda_1 + \lambda_2$ in attractors A and C is basically the same near μ_2.

As opposed to crises-induced intermittencies where attractor destruction takes place, as in our case, chaotic attractor destruction crises where intermittency is present may occur, as in the case of the two-level model for the CO_2 laser with modulated losses [29]. Here it has been found that the intersection of the stable and unstable manifolds related to saddles of period n destroys a chaotic attractor created from a saddle of period $n - 1$ and as a result a new chaotic attractor is created [30]. Therefore one may expect a jump in the dimensions of the old and new attractors. Notice that in the CO_2 laser model the strange attractors are stable for controls beyond the crises, while here the observed attractor C according to the theory [27] and our numerical computations exists just in the neighborhood of the crisis, i.e., during the formation of a new heteroclinic tangency.

On the other hand, in the context of optical phenomena for the Ikeda map [31] the coexistence of a periodic attractor and Newhouse sinks has been shown. However, here we have seen that the onset of a sink may destabilize the existing attractor in a finite interval of μ, beyond which attractor A reappears. Let us recall that our dissipative system is reversible as opposed to the above-mentioned model equations. That allowed us to predict the heteroclinic crisis in terms of the collision between the attractor and repeller. Finally, we would like to point out that due to the symmetry property S_1 there is a symmet-

ric attractor $\tilde{C}$ corresponding to attractor C. Attractor $\tilde{C}$ has been observed in our numerical calculations.

V. CONCLUSIONS

In the present paper we have studied a set of new equations that describe the long-term dynamics in a system consisting of a thin layer of two-level atoms driven by an external coherent field and a phase-conjugated mirror. Since the variables of the system are localized on the Bloch sphere, chaos occurs due to the explicit time dependence of the Rabi frequencies. This time dependence comes from the carrier frequency shift induced by the PCM on the incident probe field. Crises of attractor-merging and attractor-widening types related to the homoclinic and heteroclinic tangencies respectively occur in the present system. Crises have been studied here within the framework of optical phenomena in a dissipative system whose variables are defined on the sphere.

Two symmetries are useful in the study of this system. These are related with reversibility and half-period shift invariance of the equations. In particular, the symmetries allow us to predict the onset of a crisis of attractor-widening type, since the relevant stable and unstable manifolds are given by the attractor and repeller of the system, respectively. The stable and unstable manifolds which induce both crises are constructed. In the case of crisis of attractor-merging type we find the critical exponent by determining the eigenvalues of the saddle point whose manifolds induce the homoclinic tangency. This critical exponent is also determined by plotting the power-law scaling of the average switching time among the attractors versus a PCM gain coefficient increment. Both calculations give very close results. On the other hand, we have shown that in a crisis of attractor-widening type not only jumps in size may occur but also changes in dimension related with the destruction of the attractor in a very small interval of the control parameter. The latter is due to the collision of the previous attractor with its basin boundary, which in turn is related to the onset of new attractors induced by the tangency of the invariant manifolds. The hyperboliclike time dependence that this new attractor shows for the positive Lyapunov exponent transient indicates that the maximum expansion rate is the same in all the points on this new attractor.

ACKNOWLEDGMENTS

We are grateful for the hospitality of the Condensed Matter group at the International Centre for Theoretical Physics. We would like to thank Professor F. T. Arecchi, Professor C. Camacho, and Professor I. Procaccia for valuable discussions.

---

* Present address: Departamento de Fisica Aplicada, CINVESTAV, Merida, Yucatan, Mexico.
† Also at Instituto de Fisica, Universidade Estadual de Campinas, 13081 Campinas, S.P., Brazil.

[1] M. G. Benedict, V. A. Malishev, E. D. Trifonov, and A. I. Zaitsev, Phys. Rev. A **43**, 3845 (1991), and references therein.
[2] A. M. Basharov, A. I. Maimistov, and E. A. Manykin, Zh. Eksp. Teor. Fiz. **97**, 1530 (1990) [Sov. Phys. JETP **70**, 864 (1990)].
[3] Y. Ben-Ayreh and C. M. Bowden, J. Opt. Soc. Am. B **8**, 1168 (1991), and references therein.
[4] C. L. Pando L. and H. A. Cerdeira, Opt. Commun. **88**, 258 (1992).
[5] L. Allen and J. H. Eberly, *Optical Resonance and Two Level Atoms* (Wiley, New York, 1975).
[6] R. J. Cook and P. W. Milonni, IEEE J. Quantum Electron. **QE-24**, 1383 (1988).
[7] R. H. Abraham and H. B. Steward, Physica **21D**, 394 (1986).
[8] C. Grebogi, E. Ott, and J. A. Yorke, Phys. Rev. Lett. **57**, 1284 (1986).
[9] C. Grebogi, E. Ott, F. Romeiras, and J. A. Yorke, Phys. Rev. A **36**, 5365 (1987).
[10] W. L. Ditto *et al.*, Phys. Rev. Lett. **63**, 923 (1989).
[11] M. F. Finardi *et al.*, Phys. Rev. Lett. **68**, 2989 (1992).
[12] *Optical Phase Conjugation*, edited by R. A. Fisher (Academic, New York, 1983).
[13] J. D. Jackson, *Classical Electrodynamics* (Wiley, New York, 1962).
[14] L. Moi *et al.*, Phys. Rev. A **27**, 2043 (1983).
[15] R. Bonifacio and L. A. Lugiato, Opt. Commun. **47**, 79 (1983).
[16] A. J. Lichtenberg and M. A. Lieberman, *Regular and Stochastic Motion* (Springer-Verlag, Berlin, 1983).
[17] H. Haken, Phys. Lett. **94A**, 71 (1983).
[18] R. L. Devaney, Trans. Am. Math. Soc. **218**, 89 (1976).
[19] J. K. Moser, *Stable and Random Motion in Dynamical Systems* (Princeton University Press, Princeton, NJ, 1973).
[20] G. R. W. Quispel and J. A. G. Roberts, Phys. Lett. A **135**, 337 (1989).
[21] M. B. Sevryuk, *Reversible Systems*, Lecture Notes in Mathematics Vol. 1211 (Springer, Berlin, 1986).
[22] A. Politi, G. L. Oppo, and R. Badii, Phys. Rev. A **33**, 4055 (1986).
[23] J. M. T. Thompson and H. B. Steward, *Nonlinear Dynamics and Chaos* (Wiley, New York, 1986).
[24] E. G. Gwinn and R. M. Westervelt, Phys. Rev. A **33**, 4143 (1986).
[25] H. Ishii, H. Fujisaka, and M. Inoue, Phys. Lett. **116A**, 257 (1986).
[26] P. Grassberger and I. Procaccia, Physica **13D**, 34 (1984).
[27] J. Guckenheimer and P. Holmes, *Nonlinear Oscillations, Dynamical Systems and Bifurcations of Vector Fields* (Springer-Verlag, Berlin, 1983).
[28] C. Robinson, Commun. Math. Phys. **90**, 433 (1983).
[29] H. G. Solari, E. Eschenazi, R. Gilmore, and J. R. Tredicce, Opt. Commun. **64**, 49 (1987).
[30] I. B. Schwartz, Phys. Rev. Lett. **60**, 1356 (1988).
[31] S. M. Hammel, C. K. R. T. Jones, and J. V. Moloney, J. Opt. Soc. Am. B **2**, 552 (1985).